GEOLOGICA CARPATHICA, FEBRUARY 2020, 71, 1, 14–23 https://doi.org/10.31577/GeolCarp.71.1.2

Geoelectrically distinct zones in the crust of the Western Carpathians: A consequence of Neogene strike-slip tectonics

VLADIMÍR BEZÁK[1,✉], JOSEF PEK[2], JÁN VOZÁR[1], DUŠAN MAJCIN[1], MIROSLAV BIELIK[1,3] and ČESTMÍR TOMEK[1]

[1]Earth Science Institute of the Slovak Academy of Sciences, Dúbravská cesta 9, 840 05 Bratislava, Slovakia; ✉geofbezv@savba.sk
[2]Institute of Geophysics, Academy of Sciences of the Czech Republic, Boční II/1401, 141 31 Praha 4, Czech Republic
[3]Department of Applied and Environmental Geophysics, Faculty of Natural Sciences, Comenius University, Mlynská dolina, 842 48 Bratislava, Slovakia

(Manuscript received August 8, 2019; accepted in revised form January 8, 2020)

Abstract: Seismic reflection profile 2T is one of the best known geophysical profiles in the Carpathian region. It is very interesting from the geological point of view, because it cross-cuts all the basic tectonic units of the Western Carpathians. This profile was only interpreted by seismic methods and has never been modelled by the magnetotelluric method or compared with results of other geophysical methods. This missing study is the main objective of our paper and results in the new interpretation of the Western Carpathian crustal structure. The 2T profile can be divided into four main independent tectonic zones from an electrical conductivity viewpoint, and this is also supported by information from seismic, gravimetric and partly geothermic results. The first zone from the north is the segment of the Outer Western Carpathians with conductive sedimentary sequences of the Flysch belt overriding the non-conductive European platform. The following zone is represented by resistive migmatitic complexes of the Tatric Unit. The next zone to the south is composed from much more conductive metamorphic complexes of the Veporic Unit. The southernmost zone is characterized by very conductive structures in the whole crust. The boundaries of the zones in the geophysical cross-sections are manifested by subvertical Neogene (Neoalpine) strike-slip zones. The 2-D zones visible in the cross-sections and on the maps are the projections of the separate independent crustal segments. Older tectonic structures (mainly the Paleo-alpine and Hercynian overthrusts) are preserved inside these crustal segments.

Keywords: Western Carpathians, magnetotellurics, physically distinct zones, strike-slip tectonics.

Introduction

The deep seismic reflection profile 2T crossing the middle part of the Western Carpathian arc (Fig. 1) has provided valuable information for a better understanding of the Western Carpathian structural and tectonic development. The profile runs across all the basic tectonic units of the Outer and Inner Western Carpathians, from the Flysch Belt in the north, across the Klippen Belt and the main crustal units of the Inner Carpathians (Tatric, Veporic, and Gemeric units), to the sedimentary and volcanic Tertiary formations.

The geological interpretation of this seismic profile was published for the first time by Tomek et al. (1989). Some clarifications (Tomek 1993; Tomek & Hall 1993) and reinterpretations (Buday et al. 1991; Bielik et al. 2004) have emerged since then. Most of the interpretations were based on seismic and other geophysical methods, but the geoelectrical models provided by the magnetotelluric method have never been used to provide additional information.

Magnetotelluric (MT) measurements were carried out along the 2T profile (Varga & Lada 1988). The most complicated southern part of the profile was re-measured and interpreted again by Bezák et al. (2015). Gravimetric models are also available along the profile (e.g., Grand et al. 2002). Moreover, geothermic modelling was carried out on the profile (Majcin et al. 1998).

The 2T profile has been the subject of our recent MT new modelling (using new processing and inversion methods) and reinterpretation, which provide new and more precise identifications of the crustal elements. The main objective of this work is to contribute to the new view of the Western Carpathian crustal structure in Central Slovakia by considering information from other geophysical (mainly gravimetric, seismic and geothermic) data.

The Neoalpine tectonic style in the Carpatho-Pannonian area, namely the gradual filling of the North Penninic flysch basins by separate terranes (Carpathian block, Pelsonia, Tiszia etc.) along large strike-slip faults, is the commonly accepted setting. Our study shows the existence of separate crustal segments also within the Carpathian terrane itself and probably also within other terranes in this area, which can resolve a couple of unsolved geological problems.

Geological setting

The very complex geological structure of the Western Carpathians is the combination of remnants of Hercynian structures, the Paleo-alpine nappe system and Neoalpine block tectonics. The tectonic development of the Western Carpathians was addressed in several studies (e.g., Plašienka et al. 1997; Bezák et al. 2004). Their principal tectonic division into

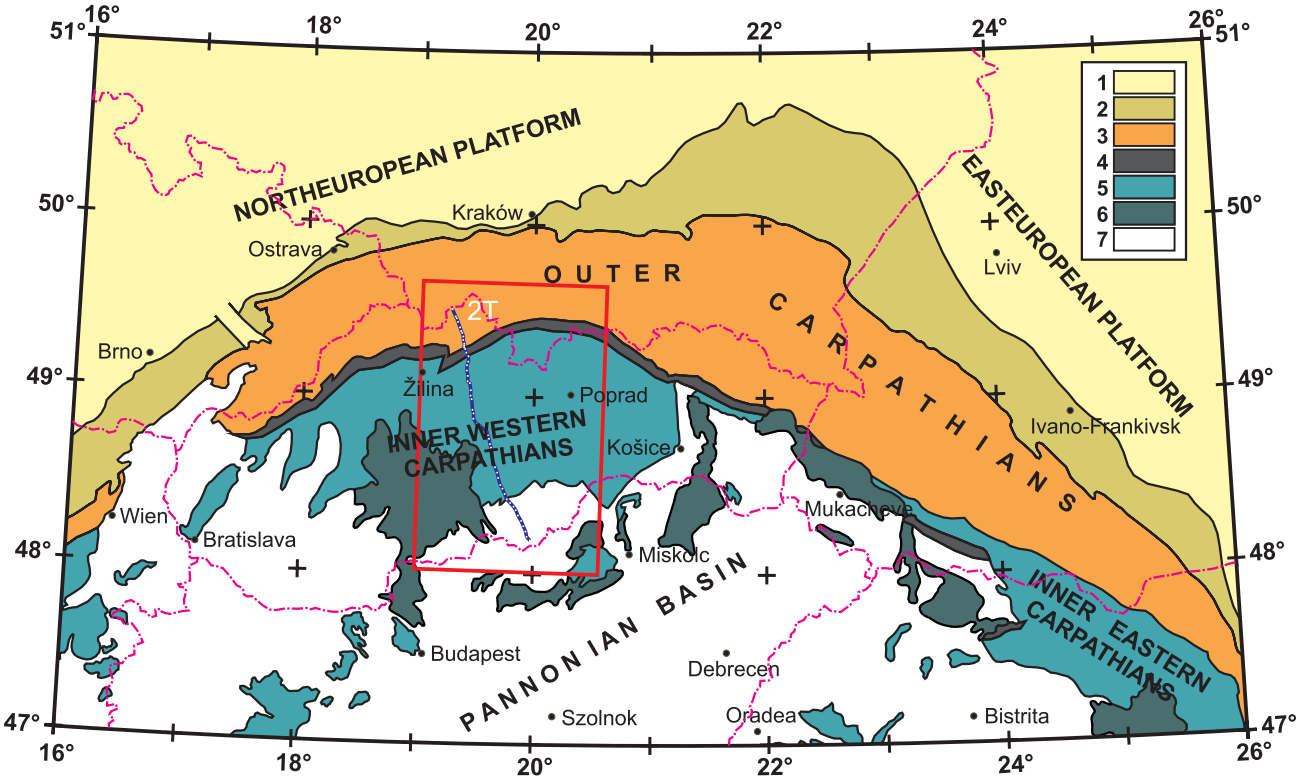

Fig. 1. Position of the 2T profile in the Carpatho–Pannonian region. The basic tectonic map was modified after Majcin et al. (2017). Key: 1 — European platform, 2 — Foredeep units, 3 — Outer Carpathian Flysch Belt, 4 — Klippen Belt, 5 — Inner Carpathian units, 6 — Neogene volcanites on the surface, 7 — Neogene and Quaternary sediments.

the Outer and Inner Carpathians after the newest tectonic map of Slovakia (Bezák et al. 2004) was explained by the youngest Neoalpine (mostly Miocene) tectonic processes, during which the flysch belt of the Outer Western Carpathians was formed. This flysch belt is overthrusted on the European platform as nappes (accretionary wedges of former subduction zones) due to the interactions of the block of the Inner Western Carpathians with the European platform. Unlike the Eastern Alps, where frontal collision with the European platform took place, the area of the Western Carpathians only manifested as an oblique collision along the curved edge of the platform. Particularly, the Neoalpine tectonic development of the Western Carpathians was studied in many works, e.g., Royden et al. (1982), Roth (1986), Csontos et al. (1992), Ratschbacher et al. (1993), Nemčok et al. (1998), Kováč et al. (1998), Sperner et al. (2002).

The Inner Western Carpathians contains the Paleo-alpine (Late Cretaceous) crustal units (Tatricum, Veporicum, Gemericum) and detached superficial Mesozoic nappes (Fatricum, Hronicum, Meliaticum, Turnaicum, Silicicum). These crustal units were built on a crystalline basement composed of fragments of the Hercynian tectonic units and the Upper Paleozoic and Mesozoic cover formations. The Hercynian tectonic units are the fundamental structural units of the Western Carpathian crust. They are mid-crustal nappes, composed of Paleozoic complexes of metamorphic rocks and granitoid bodies. The relics of Mesoalpine tectonic units occur only at the boundary of the present-day Outer and Inner Carpathians and were predominantly structurally reworked during the Neoalpine tectonic stage (i.e., the formations of the Klippen Belt). The youngest Neoalpine complexes in the Inner Western Carpathians are superimposed on the older nappe system. There are sedimentary basins with Quaternary, Neogene, Paleogene and Late Cretaceous filling and volcanic complexes of Neogene age.

The position of the seismic profile 2T in the tectonic scheme after Bezák et al. (2011) and the locations of MT sites are shown in Fig. 2. The profile traverses from the north through the Flysch belt (FB), which is separated from the Inner Carpathian units by the Klippen belt (KB). The Inner Western Carpathian block contains tectonic units from the earlier Hercynian and Paleo-alpine stages of tectonic development, mainly the crustal Paleo-alpine units of the Tatricum, Veporicum and Gemericum, which are composed of crystalline basement rocks with Mesozoic cover and superficial Mesozoic nappes. The profile also crosses some Tertiary postnappe complexes, such as basin sedimentary filling in the Liptovská kotlina, Breznianska panva and Lučenecká kotlina basins and Neogene volcanites.

MT modelling and methods

The deep seismic reflection image of the 2T profile dominantly shows the main overthrust boundaries of Paleo-alpine

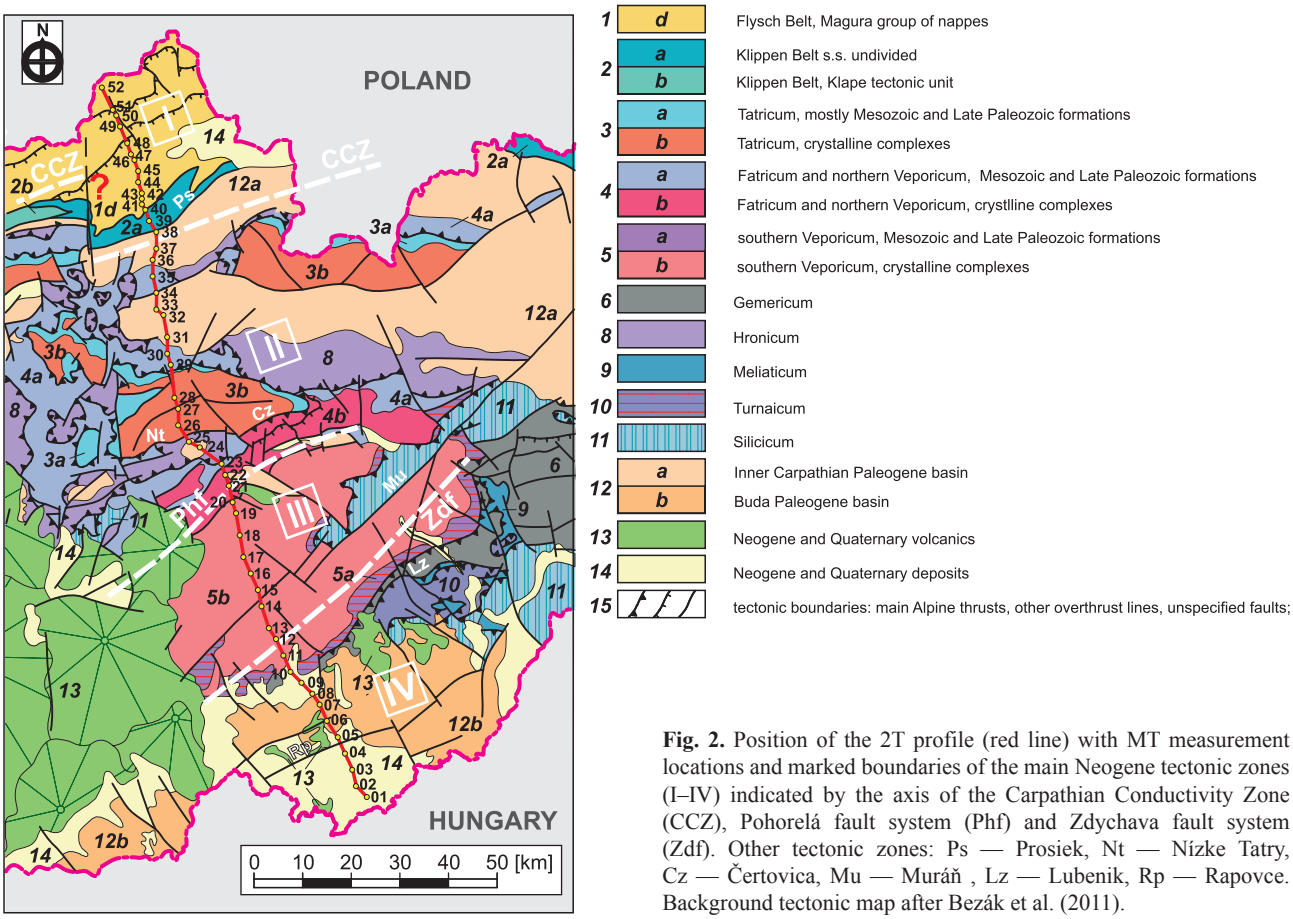

Fig. 2. Position of the 2T profile (red line) with MT measurement locations and marked boundaries of the main Neogene tectonic zones (I–IV) indicated by the axis of the Carpathian Conductivity Zone (CCZ), Pohorelá fault system (Phf) and Zdychava fault system (Zdf). Other tectonic zones: Ps — Prosiek, Nt — Nízke Tatry, Cz — Čertovica, Mu — Muráň , Lz — Lubenik, Rp — Rapovce. Background tectonic map after Bezák et al. (2011).

or Hercynian units, but their lithological compositions could not be differentiated. For this reason, MT measurements were carried out along the profile (Varga & Lada 1988) with the main objective of supplementing information about the tectonic units in terms of their conductivity properties. The southernmost, problematic portion of the profile was re-measured by our team with new broadband MT instruments (Metronix GmbH GMS-06) and processing codes (Bezák et al. 2015). Electrical conductivity, which varies over 10 orders of magnitude in common Earth materials (Haak & Hutton 1987; Bedrosian 2007), is an important physical property that plays a significant role in understanding the dynamic, compositional, and transport properties of geological units. Low conductivity anomalies suggest dry, compact, resistive rocks or a lack of deformation causing interconnected, conductive paths to arise. In contrast, high conductivity anomalies indicate compact, conductive rocks, domains of fluid accumulation, faults or interfaces containing smeared-out, macroscopically interconnected electric conductors, such as graphite, melt or sulphides, and increases in temperature.

The MT measurements along the 2T profile were modelled using common modelling and inversion methods, and we constructed a geoelectrical model of the underlying geological units. The final model (Fig. 3) allows us to identify the regional geoelectrical structures, meaning the geological units with contrasting resistivity/conductivity parameters. The MT model reveals the positions and structures of deep crustal tectonic units and identifies the major deep fault zones.

Two MT data sets were available for modelling the crustal conductivity structure along the 2T profile, specifically: (i) broad-band data (periods from 0.05 to approximately 500 s) from earlier measurements by ELGI Budapest and Geofyzika Brno in the 1980s at 52 sites obtained along the 2T profile, which is approximately 150 km long and ranges between 48.20°N, 19.98°E in the south-east and 49.49°N, 19.25°E in the north-west (Varga & Lada 1988); and, (ii) broad-band MT measurements (periods from 0.001 to approximately 100 s) conducted together by the Geophysical Institutes from the Czech and Slovak Academy of Sciences in 2013 at 10 sites along the southernmost, 25-km-long section of the profile, ranging between 48.28°N, 19.93°E in the south and 48.49°N, 19.73°E in the north (Bezák et al. 2016). The MT data were of acceptably good quality, except for a few stations in the section crossing the Nízke Tatry Mts. (between 50–70 km, Fig. 3), where an increased level of industrial noise over high-resistivity basement affected the MT curves, especially at longer periods.

The standard dimensionality and directionality analysis of the MT data (Simpson & Bahr 2005) was carried out along the whole profile, as well as on several profile sections aligned with underlying large-scale geological zones. The dimensionality analysis shows that upper crustal structures may be

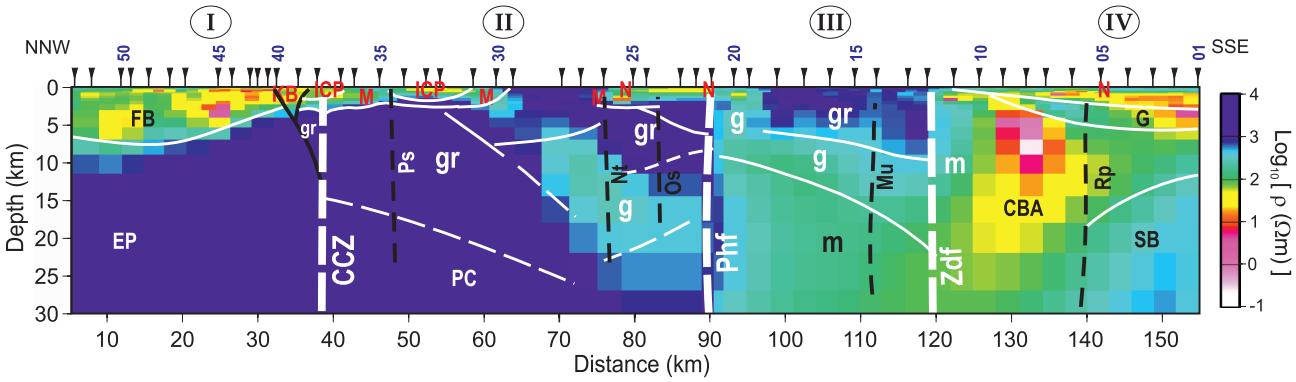

Fig. 3. Geoelectrical model of the 2T profile and their geological interpretation. EP — European platform, FB — Flysch belt, PC — Pieninic crust, KB — Klippen belt, M — Mesozoic complexes, ICP — Inner Carpathian Paleogene, N — Neogene sediments and volcanites, G — Gemeric complexes, SB — southern Cadomian basement, CBA — crystalline basement altered, gr — Hercynian granitoids and migmatitic complexes, g — Hercynian gneisses, m — Hercynian mica-schists. Main tectonic zones: CCZ — Carpathian Conductive Zone axis, Phf — Pohorelá fault system, Zdf — Zdychava fault system. Faults of second order: Ps — Prosiek, Nt — Nízke Tatry, Os — Osrblie, Mu — Muráň, Rp — Rapovce.

reasonably well-approximated by a 2-D model, with stronger 3-D effects indicated beneath the Nízke Tatry Mts. region (section between 50 and 70 km on the profile, Bezák et al. 2016) and at the transition from the Veporicum to the Tertiary sediments of the Lučenská kotlina basin (between 110 and 130 km). In the Nízke Tatry Mts. region, the effects of cultural noise cannot be excluded. The basic dimensionality indicators indicate that a large-scale 2-D model with moderate 3-D distortions may be considered. Spatial distributions of both the classical Swift's skew and Bahr's phase sensitive skew along the profile are shown by contour maps in Supplementary Fig. S1.

Structural strike analysis was carried out by fitting a Groom & Bailey (1989) model of a 3-D local/2-D regional structure to the MT data by employing a Monte Carlo procedure (Červ et al. 2010). Although the decomposition parameters are scattered considerably for individual sites and periods, they yield reasonably stable directional patterns at several sites if multiple periods are merged and analysed simultaneously. From a series of multi-site, multi-frequency decomposition experiments (Bezák et al. 2015, 2016), we can summarize that: (i) large-scale strike patterns differ between the southern and northern parts of the 2T profile, specifically roughly between 0 and 75 km (northern part) and 75 to 150 km (southern part), respectively; (ii) the strikes are highly scattered for the shallowest part of the profile, down to a Bostick penetration depth of approximately 1 km, estimated from the average impedance data; (iii) in the northern part (2T North), strike estimates clustered around N63°E (with ±90° ambiguity) for Bostick depths corresponding to the upper crust (1 to 10 km) and around N56°E for depths between 10 and 30 km; (iv) on the southern subprofile (2T-South), strike estimates were close to N41°E (±90°) for the Bostick depth range of 1 to 10 km, and around N45°E for depths between 10 and 30 km. Based on these strike estimates, we divided the profile into two parts and carried out subsequent modelling experiments for 2T-North, with a common 2-D strike of N60°E, and 2T-South, with a common strike of N45°E. Outputs of the regional strike analysis for individual MT sites and for the N and S sections of the 2T profile are shown for the above two Bostick depth ranges in Supplementary Fig. S2.

A series of inversions of the MT data was carried out by employing the 2-D non-linear conjugate gradients inverse algorithm by Pek et al. (2012), separately, to model 2T-North and 2T-South, using their respective 2-D strikes. Models for both sections consisted of 187×40 (=7480) rectangular cells, but some cells in the models were aggregated into larger blocks, especially in remote and deep parts of the models, so that the number of distinct conductivity domains was reduced to 2238 in each model. The inverse runs were carried out with data for about 50 periods from the range of 0.05 to 700 s at each site, but various restriction and decimation schemes were used in different experiments to reduce the computation time. As the induction arrows were scattered and inconsistent throughout that period range, we ran the inversions with the impedances only. To avoid unrealistically small data variances, a common error floor of 5 % and 10 % of the maximum impedance magnitude was applied to the principal and secondary impedance data, respectively. To minimize the destructive effect caused by rotations of the experimental data into the strike direction, we inverted the complete impedance tensor data in the observation (NS–EW) frame and compared them with the rotated model responses.

As a rule, the inversions were carried out in several steps, starting from a homogeneous half-space (100 Ohm.m) and adjusting the initial models in the course of the inversion to restrict zones of persistently poor convergence. Additional tests were also performed considering anisotropic conductivities in the model or strong galvanic distortions in the data but no distinguished or systematic structural features could be concluded in the final models from those tests. To assess the reliability of the models, we tested the persistence of the main conductivity domains by repeated inversion runs. The model shown in Fig. 3 is a stitched version of the inversion results,

with RMS values of 3.2 for the northern sub-profile and 1.6 for the southern part of 2T. Comparison of the observed and modelled data is presented in the form of apparent resistivity/phase pseudo sections in Supplementary Fig. S3.

A few sections of the model must be handled with caution. In particular, the high-resistivity, emerging basement below the Liptovská kotlina basin and the Nízke Tatry Mts. section of the profile (between 35 and 65 km in Fig. 3) may be partly due to the near-field source effects of industrial distorters in this region. The largely undifferentiated internal structure of this massive resistor, as well as the lack of conductivity features that would suggest a deep source of the well-known Carpathian Conductivity Zone (between 30 and 40 km on the profile in Fig. 3 according to long-period induction arrows), make that interpretation even more likely. Another debatable feature is the south-dipping decreased resistivity zone between 60 and 85 km on the profile, which is, in fact, only required by the northern data, while the data from 2T-South rather suggest a simple resistive block throughout the whole crust. As the model strike changes at this position, reliable verification of this zone is difficult.

Geological interpretation of the MT model

The primary MT modelling results along the 2T profile are geologically interpreted in Fig. 3. The 2T profile can be divided into four zones from an electrical conductivity viewpoint. Zone I of the presented model stands out due to the contrast of the conductive sedimentary sequences of Flysch belt (FB) against the non-conductive European platform (EP), which consists of the Cadomian crystalline basement (e.g., Dudek 1980). The platform significantly bends upward towards the south, namely towards the supposed former subduction zone. This flexure is also visible in the seismic profile (Tomek et al. 1989, Fig. 4). Its explanation remains unclear. It might be an effect of bending in front of the former subduction zone, where the down-bending part of the platform was amputated. The southern border of the platform represents the Carpathian Conductive zone (CCZ, Kucharič et al. 2013). The CCZ is not visible in the presented MT model and seems to be drowned out by the industrial noise in the telluric records although its existence in this area was shown by Jankowski et al. (1985) and Červ et al. (2001) from long period geomagnetic induction data (induction arrows). This might also be caused by 3-D effects in the CCZ geoelectrical image, which cannot be mapped by 2-D modelling. The CCZ is more clearly visible in the MT models in western Slovakia (Bezák et al. 2014). Particularly in the area of the 2T profile there are differences in the position of the CCZ in Jankowski et al. (1985) and Červ et al. (2001) works. The explanation for these differences could be the offset of the CCZ along the perpendicular fault (Fig. 2).

As suggested by the geoelectrical model in the western (Bezák et al. 2014) and eastern parts of Slovakia (Majcin et al. 2018), the Klippen Belt (KB) seems to be a shallow structure. It seems that the KB, with a part of the Tatricum, here exists in a flower structure over the CCZ. This flower structure is much more pronounced in the western part of Slovakia (Bezák et al. 2014).

Zone II consists mainly of crystalline complexes of the Tatricum (mainly granitoids and orthogneisses) and it is equally resistive as the basement of the EP in zone I. These two zones with resistive blocks are suggested by smooth change in the magnetic map (Fig. 5) because the Cadomian crystalline complexes of the EP create magnetic anomalies due to the large presence of mafic rocks.

In the northern part of zone II, the sediments of the Inner Carpathian Paleogene basin and Mesozoic series are manifested as shallow, relatively conductive structures above the resistive crystalline rocks. The deepest structures here are composed of the supposed Pienninic crust (PC), on which the crystalline basement of the Tatricum was superimposed during the Mesoalpine stage of its tectonic evolution (Bezák et al. 2004).

The southernmost part of zone II shows the presence of resistive units formed by the migmatitic crystalline complexes of the Veporicum Ľubietová zone and overlying Mesozoic complexes. This area mainly consists of poorly conductive orthogneisses and Mesozoic complexes. The higher-conductivity areas in this section of the profile have been presented only in the shallow basin structure of the Breznianska kotlina

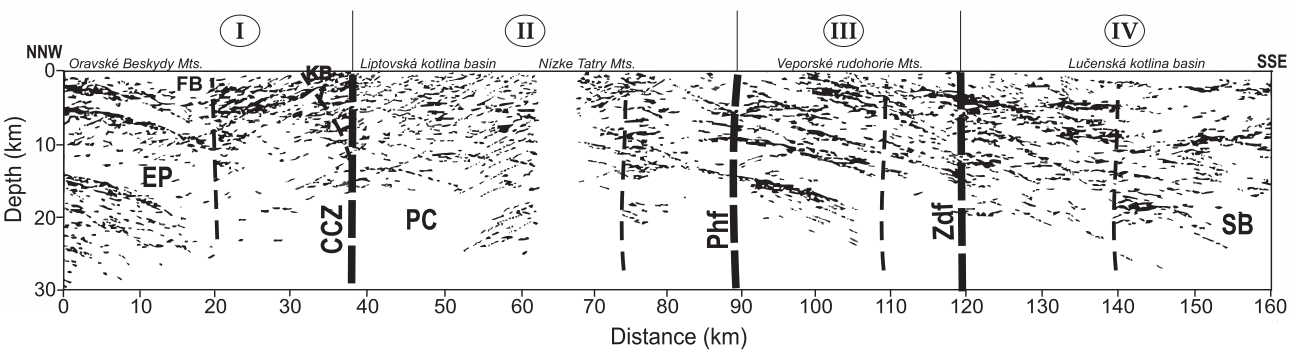

Fig. 4. Seismic profile 2T (Tomek et al. 1989). Explications see Fig. 3. Thin dashed lines — faults of second order.

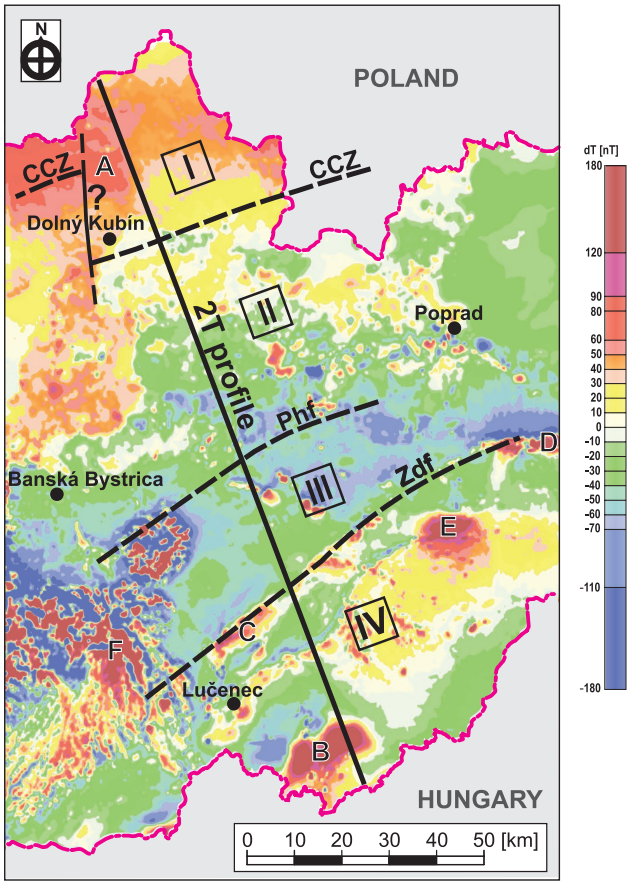

Fig. 5. Position of the 2T profile with main geoelectrical zones and main magnetic anomalies in the Magnetic map section after Kubeš et al. (2010). Magnetic anomalies: A — European platform, B — southern Cadomian basement, C — mica-schists, D — mafic Paleozoic rocks, E — Rochovce Cretaceous granite, F — neovolcanites.

basin and neovolcanites. The southern border of zone II is represented by a steep fault zone, projected as the Pohorelá fault system (Phf) onto the surface (Bezák et al. 2004). This fault is well-known in Carpathian geology and it is characterized by the presence of a huge amount of mylonites. The thicknesses of these mylonites indicate a long distance of translation along the fault (Bezák 2002). The great horizontal translation on this fault separates two diametrically different Mesozoic cover complexes of the Veporicum (North Veporic shallow-sea and South Veporic deep-sea facies). This fault divides resistive crustal segments in the North (I, II) from non resistive crustal segments (III, IV) in the South and it also represents the southern border of the significant gravity low (Fig. 6), which is well-known as the Western Carpathian gravity low (CGL) after Tomek et al. (1979).

Southward from the Pohorelá fault, we recognized geoelectrical zone III, which is more heterogeneous in comparison to the zone II. The change in physical properties between these two zones is very rapid and we interpret it as a boundary between these zones in the form of a young, steep fault zone. In zone III, the Veporic crystalline units, which comprise slightly conductive metamorphic complexes (mostly mica-schists), prevail. These structures, in the central part of zone III are overlain by a substantially resistive complex of granitoids and gneisses. This granitoid zone was originally tectonically superposed during the main Hercynian collision in the Paleozoic era (Bezák et al. 1997). The southern border of the zone III represents the very important strike-slip Zdychava fault (Zdf) with a wide mylonitic zone notably observed from geological mapping, such as that of Bezák et al. (2004). This fault separates the migmatite and granite rich complexes of the Hercynian middle lithotectonic unit and mica-schists of the lower lithotectonic unit (Bezák et al. 1997), which are extruded on this transpressional structure.

A sharp change in the conductivity parameters between zones III and IV is obvious. The higher conductivity values for the shallower structures are associated with Neogene sediments (N) and Gemeric metasediments (G) containing graphitic shales. In the deeper crust, there are mostly Veporic crystalline rocks, altered by hydrothermal processes (CBA) connected with Tertiary volcanism; thus, for that reason, they exhibit relatively larger conductivity value. The high crustal conductivity is caused by a disruption in the crust by young Tertiary and Quaternary tectonic and volcanic activity connected with hydrothermal processes (Bezák et al. 2015). Zone IV is greatly influenced by younger volcanic processes, which

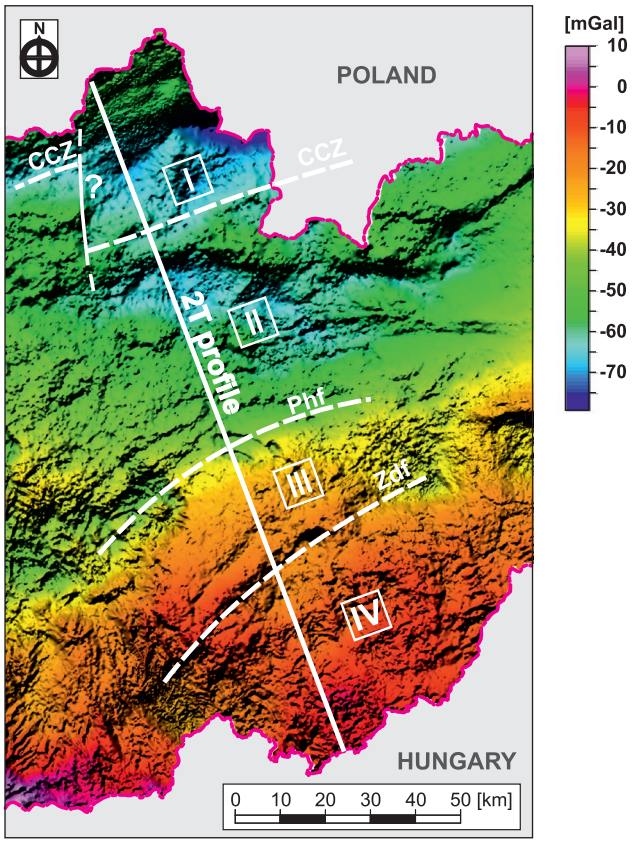

Fig. 6. Position of the 2T profile with main geoelectrical zones in the part of Complete Bouguer Anomaly map after Pašteka et al. (2017).

homogenize almost all physical differences among the units, except the supposed southern Cadomian basement (SB) in the southernmost part. This SB is a Cadomian fragment (Bezák et al. 1997), its existence indicated by xenoliths, which were brought to the surface by the basalt volcanoes in this area. Evidence for its existence also emerged from geophysical data, specifically, from a magnetic anomaly (Kubeš et al. 2010, Fig. 5) and the heavier crust in the gravity model (Grand et al. 2002, Fig. 7) and Slovak Bouguer gravity anomaly map (Pašteka et al. 2017, Fig. 6).

The boundaries of all geoelectrically distinct zones (marked as I–IV) are subvertical and visible in other geophysical models (see Figs. 4, 7). All older tectonic structures (mainly overthrusts) are preserved inside the zones; however, young tectonic segmentation has significantly affected their continuity. We interpret the borders of the geoelectrical zones in crustal blocks as Neogene (Neoalpine) shear zones (strike-slip faults).

The comparison of the MT model with other geophysical models: a discussion

The division of the Western Carpathian crust into four basic physically different zones is supported also with other geophysical methods (seismic, gravimetric, magnetic, partly geothermic).

Seismic profile (Fig. 4), taken from the paper of Tomek et al. (1989), shows the internal structures of the zones in their subhorizontal overthrust structures. All interpretations accentuate only overthrust tectonics, which is quite understandable since the vertical interfaces are not directly visible in the primary seismic analysis. Apart from the Alpine overthrusts, it is also possible to identify the traces of Hercynian overthrusts based on seismic profile (Bielik et al. 2004). However, recent studies (e.g., Ratschbacher et al. 1993; Bezák 2002; Marko et al. 2017) have shown the important role of young translations along steep faults in the geological evolution of the Western Carpathians. These vertical interfaces can also be identified in the seismic cross-section as a discontinuity in the subhorizontal seismic reflections. The most notable can be seen at the boundaries of the distinct geoelectric zones I–IV, which provide support for the validity of the existence of these zones. There are also noticeable differences in the delamination of the crust, which is significantly greater in zone III than in zone II.

For the next comparison with the MT model, we have chosen the gravity model along the 2T profile and its geological interpretation (Grand et al. 2002). The density model exhibits relatively small density differences between the major tectonic units investigated along the 2T profile, but the differences between the geoelectric zones I–IV (Fig. 7) are still visible. The model shows the lighter flysch sediments overlying the relatively dense EP, lighter granitic mass of the Tatricum block (zone II), denser metamorphic mass of the Veporicum in the zones III and IV with a relatively denser mass of the Cadomian block in the southernmost part.

The most dominant feature of the gravity observed in the newly completed Bouguer anomaly map of Slovakia (Pašteka et al. 2017) in the 2T surrounding is CGL in the N part (Fig. 6). Based on the density model of the 2T profile (Bielik 1995) and the interpretation of the stripped gravity map (Makarenko et al. 2002), it was found that the source of the CGL is the superposition of the gravity effects of two different tectonic units. The first part of the CGL (zone I) observed over the Outer Western Carpathians is due to the low density of the Palaeogene sedimentary infill of the Flysch belt and the Neogene sedimentary infill of the Carpathian Foredeep. These sediments suppress the gravitational effect of the heavier Cadomian crust of the EP, which is clearly visible in the map of magnetic anomalies (Kubeš et al. 2010, Fig. 5).

The second part of the CGL extends in zone II. The sources of this part of the CGL are the Hercynian crystalline rocks (mostly granitic and migmatitic complexes) of the upper Hercynian lithotectonic unit after Bezák et al. (1997), which now belong mostly to the Alpine Tatric unit. This tectonic unit reaches very large thicknesses (nearly 20 km), and its average

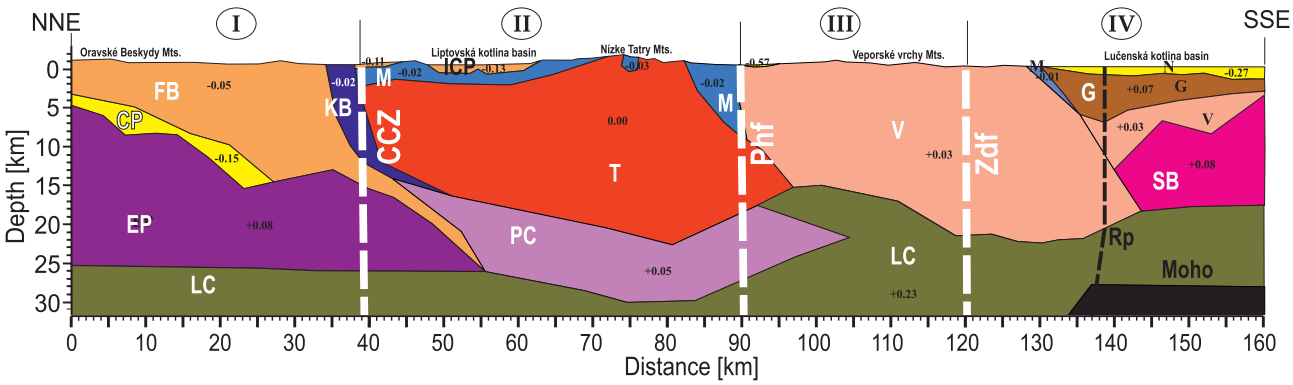

Fig. 7. Gravimetric model after Grand et al. (2002) along 2T profile. CP — platform cover, T — Tatric Unit, V — Veporic Unit, LC — lower crust, other explications see Fig. 3.

density is less than the average density of the crust. It is suggested that the density difference between them is approximately 0.20 g.cm^{-3}. The granitic complexes of the Tatric Unit mask the gravitational impact of the denser Cadomian Pieninic crust (PC), over which the Tatric Unit has probably been overthrusted (see Figs. 3, 7, 8).

Following the Complete Bouguer Anomalies (CBA) map (Fig. 6) and gravimetric model (Fig. 7), the density-distinct crustal zones III and IV comprise significantly denser rock complexes (approximately 0.1 g.cm^{-3}), which indicates their significantly different geological compositions than previous ones (I and II). A sudden change in the gravity model and in the CBA map on the interface between zones II and III can only be explained tectonically by the convergence of geologically different crustal segments. The density interface between crustal segments II and III is subvertical and it is identical with the boundary between geoelectrical segments II and III in MT model (Fig. 3). The crust in zones III and IV is built up mainly from the gneiss and mica-schist complexes of the middle and lower Hercynian units (Bezák et al. 1997), which became part of the Veporic Unit during the Alpine orogeny.

Based on geothermal modelling results along the profile 2T (Majcin et al. 1998) the differences between the recognized four geoelectric zones can also be noted in the thickness of the lithosphere. The greatest thickness of lithosphere occurs in the zone I (EP), whereas zones II and III are thinner with typical values about 100 km. The lithosphere thickness increases up to 150 km in the direction to the northern end of the profile and the greatest gradient exists at the CCZ position. Furthermore, the shift in the Moho depth at this boundary is visible in some other geophysical models (Hrubcová et al. 2010). Zone IV is very specific in relation to the lithosphere–asthenosphere boundary (LAB) shape. According to the interpretation of geothermal model data and other known geophysical data (Babuška & Plomerová 1988; Praus et al. 1990; Majcin 1993; Majcin et al. 1998), this area contains a doubled lithosphere, which disappears towards the south into the asthenolith, below the Pannonian basin realm.

The conductive structures of the entire crust in the MT profile correspond to the area of volcanic activity. This area is characterized by terrestrial heat flow density increasing southward from about 60 mWm^{-3} up to 90 (Majcin et al. 2017), resulting from the assumption of partially melted masses at a depth of 70–80 km (Majcin et al. 1998). The lithosphere doubling is interpreted in this model as a relic of Mesozoic subduction processes (also potentially containing the remains of the Meliata oceanic suture). All of these signs distinguish zone IV from zone III, which is why we consider it a separate Neoalpine block.

The Gemeric complexes and Cadomian basement in zone IV are rare in the structure of the Western Carpathians; thus, the original position of crustal segment IV before the Neoalpine shifting is very unclear. These rocks exhibit similarities with some complexes in the Upper Austroalpine unit of the Eastern Alps (Vozár et al. 2010), Cadomian basement exists in the Pelso unit, which lies to the South of the Hurbanovo fault (Bezák et al. 2004). Thus it is possible that the Rapovce fault (Rpf) in segment IV relates to the Raba–Hurbanovo–Diosjeno fault system.

The aforementioned differences in the physical characteristics of individual zones are caused by the different compositions of older tectonic units included in the new Neoalpine crustal segments (terranes). Neogene terranes do not respect the boundaries of the Paleo-alpine Cretaceous units (Tatricum, Veporicum, Gemericum, and superficial nappes), but these units are preserved within terranes in their original superposition. Each of these terranes were derived from a different paleotectonic area, and each underwent a different level of influence from

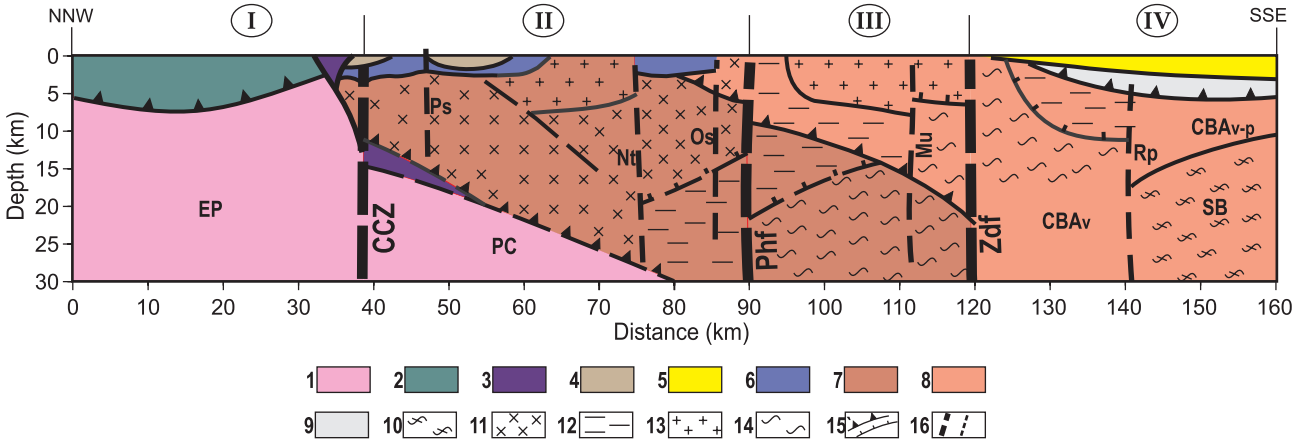

Fig. 8. Schematic tectonic profile of the Western Carpathians modified on the basis of geophysical models. Key: 1 — Cadomian crust of EP and PC, 2 — Flysch belt, 3 — Klippen belt, 4 — Inner Western Carpathian Paleogene, 5 — Neogene sediments and volcanites, 6 — Mesozoic complexes. Paleo-alpine crustal tectonic units: 7 — Tatricum, 8 — Veporicum, 9 — Gemericum. Hercynian tectonic units in the frame of the Alpine tectonic units: 10 — southern Cadomian basement, 11 — Upper lithotectonic unit, 12 — Middle lithotectonic unit, 13 — Hercynian granitoids, 14 — Lower lithotectonic unit. Tectonic boundaries: 15 — Alpine overthrust zones (up), remnants of Hercynian thrusting (down), 16 — left main Neoalpine shear zones, right Neoalpine faults of the second order (for definitions of the faults see Fig. 3). Altered crystalline basement: CBAv — in the Veporic Unit, CBAv-p — in the Veporicum or Pelso unit.

younger processes, which are mainly connected with volcanic activity.

As a conclusion of the presented geophysical models and discussed geological interpretations, we have modified the previous schematic tectonic profile across the Western Carpathians in the Tectonic map of Bezák et al. (2004). The new scheme is presented in Fig. 8.

Conclusion

The crustal structure of the Western Carpathians is interpreted based on a new magnetotelluric modelling along the seismic profile 2T situated in central Slovakia with the help of supplementary seismic, gravity, geothermal and partly magnetic data. This modelling shows that within the Carpathian block itself physically contrasting crustal segments exist. Thus, an oblique collision of the Western Carpathians with the European Platform seems to have been complicated and to have occurred by the gradual shifting of various crustal segments with different geological composition along subvertical shear-zones. We interpret these structures as Neoalpine strike-slip faults, along which compositionally distinct parts of the crust with contrasting physical parameters were juxtaposed in the present-day Western Carpathians.

Four basic zones can be identified in the crustal structure of the Western Carpathians. In the north there is a zone of the European Platform with overthrust flysch nappes, which is manifested as a resistive platform below conductive sediments. This segment of the platform is characterized by heavy mass and it is more magnetic. Further to the south, a less dense and geoelectrical highly resistive zone is present, composed of mostly granitic and migmatitized Hercynian complexes now a part of the Paleo-alpine Tatric Unit. These first two zones form the so-called Carpathian gravity low. Further to the south, there is a third zone of geoelectrically less resistive and gravimetrically denser rocks composed of Hercynian gneissic and mica-schist complexes as a part of the Paleo-alpine Veporic unit, in seismic cross-section markedly tectonically laminated. Finally, the southernmost physically distinctive zone is characterized by high conductivity throughout the crust caused by Neogene volcanism and hydrothermal activity, which masks the distinct physical properties of the tectonic units composing this zone.

Acknowledgements: The work was accomplished with partial support from grants by the APVV agency by means of project APVV 16-0482 and APVV 16-0146, and the Slovak Grant Agency VEGA by means of project 2/0006/19. The research has also been financed by the program SASPRO (1947/03/01-b) and was co-funded by the People Programme (Marie Curie Actions 7FP, grant agreement REA no. 609427-SK) and co-financed by the Slovak Academy of Sciences. The authors would like to thank both reviewers for their very helpful suggestions and comments that have improved the final manuscript.

References

Babuška V. & Plomerová J. 1988: Subcrustal continental lithosphere: a model of its thickness and anisotropic structure. *Phys. Earth Planet Inter.* 51, 130–132.

Bedrosian P.A. 2007: MT+, integrating magnetotellurics to determine earth structure, physical state, and processes. *Surveys in Geophysics* 28, 121–167. https://doi.org/10.1007/s10712-007-9019-6

Bezák V. 2002: Hercynian and Alpine strike-slip tectonics – a dominant element of tectonic development of the Inner Western Carpathians. *Geologica Carpathica* 53, 17–22.

Bezák V., Jacko S.st, Janák M., Ledru P., Petrík I. & Vozárová A. 1997: Main Hercynian lithotectonic units of the Western Carpathians. Geological evolution of the Western Carpathians. *Geocomplex*, Bratislava, 261–269.

Bezák V., Broska I., Ivanička J., Reichwalder P., Vozár J., Polák M., Havrila M., Mello J., Biely A., Plašienka D., Potfaj M., Konečný V., Lexa J., Kaličiak M., Zec B., Vass D., Elečko M., Janočko J., Pereszlényi M., Marko F., Maglay J. & Pristaš J. 2004: Tectonic map of the Slovak republic 1:500 000. *ŠGÚDŠ*, Bratislava.

Bezák V., Biely A., Elečko M., Konečný V., Mello J., Polák M. & Potfaj M. 2011: A new synthesis of the geological structure of Slovakia – the general geological map at 1:200 000 scale. *Geol. Quarterly* 55, 1–8.

Bezák V., Pek J., Vozár J., Bielik M. & Vozár J. 2014: Geoelectrical and geological structure of the crust in Western Slovakia. *Studia Geophysica et Geodaetica* 58, 473–488. https://doi.org/10.1007/s11200-013-0491-9

Bezák V., Pek J., Majcin D., Bučová J., Šoltis T., Bilčík D. & Klanica R. 2015: Geological interpretation of magnetotelluric sounding in the southern part of seismic profile 2T (Central Slovakia). *Contributions to Geophysics and Geodesy* 44, 4, 329–339. https://doi.org/10.1515/congeo-2015-0009

Bezák V., Pek J., Vozár J., Bielik M. & Majcin D. 2016: Magnetotelluric and gravity modelling of crustal structures in the northern Slovakia (Western Carpathians). In *16th SGEM conference proceedings* 1, 3, 373–380. https://doi.org/10.5593/SGEM2016/B13/S05.047

Bielik M. 1995: Continental convergence in the Carpathian region by density modelling. *Geologica Carpathica* 46, 3–12.

Bielik M., Šefara J., Kováč M., Bezák V. & Plašienka D. 2004: The Western Carpathians – interaction of Hercynian and Alpine processes. *Tectonophysics* 393, 63–86. https://doi.org/10.1016/j.tecto.2004.07.044

Bostick E.X. 1977: A simple almost exact method of MT analysis. Workshop on Electrical Methods in Geothermal Exploration, *U.S. Geol. Surv.*, Contract No. 14080001-8-359.

Buday T., Bezák V., Potfaj M. & Suk M. 1991: Discussion to interpretation of reflex seismic profiles in Western Carpathians [Diskuse k interpretaci reflexních seizmických profilů v Západných Karpatech]. *Mineralia Slovaca* 23, 3–4, 275–276 (in Czech).

Červ V., Kováčiková S., Pek J., Pečova J. & Praus O. 2001: Geoelectrical structure across the Bohemian Massif and the transition zone to the West Carpathians. *Tectonophysics* 332, 201–210. https://doi.org/10.1016/S0040-1951(00)00257-2

Červ V., Pek J. & Menvielle M. 2010: Bayesian approach to magnetotelluric tensor decomposition. *Annals of Geophysics* 53, 2, 21–32. https://doi.org/10.4401/ag-4681

Csontos L., Nagymarosi A., Horváth F. & Kováč M. 1992: Tertiary evolution of the intra-Carpathian area: a model. *Tectonophysics* 208, 221–241. https://doi.org/10.1016/0040-1951(92)90346-8

Dudek A. 1980: The crystalline basement block of the Outher Carpathians in Moravia: Bruno-Vistulicum. *Rozpr. Čs. Akad. Vied* 90, 8, 1–85.

Grand T., Šefara J., Bielik M., Bezák V. & Paštéka R. 2002: Reinterpretation of gravimetric data in the Western Carpathians. *Krystalinikum* 28, 103–108.

Groom R.W. & Bailey R.C. 1989: Decomposition of magnetotelluric impedance tensors in the presence of local three-dimensional galvanic distortion. *J. Geophys. Res.* 94, 1913–1925.

Haak V. & Hutton R. 1987: Electrical resistivity in continental lower crust. *Geological Society, London, Special Publications* 24, 1, 35–49. https://doi.org/10.1144/GSL.SP.1986.024.01.05

Hrubcová P., Środa P., Grad M., Geissler W.H., Guterch A., Vozár J. & Hegedüs E. 2010: From the Variscan to the Alpine Orogeny: crustal structure of the Bohemian Massif and the Western Carpathians in the light of the SUDETES 2003 seismic data. *Geophys. J. Int.* 183, 611–633. https://doi.org/10.1111/j.1365-246X.2010.04766.x

Jankowski J., Tarlowski Z., Praus O., Pecova J. & Petr V. 1985: The results of deep geomagnetic soundings in the West Carpathians. *Geophys. J. R. Astr. Soc.* 80, 561–574.

Kováč M., Nagymarosy A., Oszczypko N., Ślączka A., Csontos L., Marunteanu M., Matenco L. & Márton E. 1998: Palinspastic reconstruction of the Carpathian-Pannonian region during the Miocene. In: Rakús M. (Ed.): Geodynamic Development of the Western Carpathians. *GSSR,* Bratislava, 189–217.

Kubeš P., Bezák V., Kucharič Ľ., Filo M., Vozár J., Konečný V., Kohút M. & Gluch A. 2010: Magnetic field of the Western Carpathians (Slovakia): reflection structure of the crust. *Geol. Carpath.* 61, 437–447. https://doi.org/10.2478/v10096-010-0026-z

Kucharič Ľ., Bezák V., Kubeš P., Konečný V. & Vozár J. 2013: New magnetic anomalies of the Outer Carpathians in NE Slovakia and their relationship to the Carpathian Conductivity Zone. *Geol. Quaterly* 57, 1, 123–134. https://doi.org/10.7306/gq.1079

Majcin D. 1993: Thermal state of the west carpathian lithosphere. *Studia Geophysica et Geodaetica* 37, 4, 345–364.

Majcin D., Dudášová V. & Tsvyashchenko V.A. 1998: Tectonics and temperature field along the carpathian profile 2T. *Contrib. Geophys. Geod.* 28, 2, 107–114.

Majcin D., Král M., Bilčík D., Šujan M. & Vranovská A. 2017: Thermal conditions for HDR sources in the region of Slovakia. *Contrib. Geophys. Geod.* 47, 1, 1–22. https://doi.org/10.1515/congeo-2017-0001

Majcin D., Bezák V., Klanica R., Vozár J., Pek J., Bilčík D. & Telecký J. 2018: Klippen Belt, Flysch Belt and Inner Western Carpathian Paleogene basin relations in the Northern Slovakia by magnetotelluric imaging. *Pure Appl. Geophys.* https://doi.org/10.1007/s00024-018-1891-0

Makarenko I., Legostaeva O., Bielik M., Starostenko V., Dérerová J. & Šefara J. 2002: 3D gravity effects of the sedimentary complexes in the Carpathian-Pannonian region. *Geol. Carpath.* 53, special issue.

Marko F., Andriessen P.A.M., Tomek Č., Bezák V., Fojtíková L., Bošanský M., †Piovarči M. & Reichwalder P. 2017: Carpathian Shear Corridor – a strike-slip boundary of an extruded crustal segment. *Tectonophysics* 703–704, 119–134. https://doi.org/10.1016/j.tecto.2017.02.010

Nemčok M., Pospíšil L., Lexa J. & Donelick R.A. 1998: Tertiary subduction and slab break-off model of the Carpathian-Pannonian region. *Tectonophysic*s 295, 307–340. https://doi.org/10.1016/S0040-1951(98)00092-4

Pašteka R., Zahorec P., Kušnirák D., Bošanský M., Papčo J., Szalaiová V., Krajňák M., Marušiak I., Mikuška J. & Bielik M. 2017: High resolution Slovak Bouguer gravity anomaly map and its enhanced derivative transformations: new possibilities for interpretation of anomalous gravity fields. *Contrib. Geophys. Geod.* 47, 2, 81–94. https://doi.org/10.1515/congeo-2017-0006

Pek J., Santos F.A.M. & Li Y. 2012: Non-Linear Conjugate Gradient Magnetotelluric Inversion for 2-D Anisotropic Conductivities. In: Börner R.-U. & Schwalenberg K. (Eds.): Proceed. 24th Colloq. Electromagnetic Depth Investigations, Neustadt/Weinstr, 26.9.–30.9.2011. *DGG*, 187–206

Plašienka D., Grecula P., Putiš M., Kováč M. & Hovorka D. 1997: Evolution and structure of the Western Carpathians: an overview. In: Grecula P. (Ed.): Geological Evolution of the Western Carpathians. *Mineralia Slovaca*. Monograph. *State Geological Institute of Dionýz Štúr*, Bratislava, 7–24.

Praus O., Pěčová J., Petr V., Babuška V. & Plomerová J. 1990: Magnetotelluric and seismological determination of lithosphere-asthenosphere transition in Central Europe. *Phys. Earth. Planet. Inter.* 60, 212–228. https://doi.org/10.1016/0031-9201(90)90262-V

Ratschbacher L., Frisch W., Linzer H.G., Sperner B., Meschede M., Decker K., Nemčok M., Nemčok J. & Grygar R. 1993: The Pieniny Klippen Belt in the Western Carpathians of northeastern Slovakia: structural evidence for transpression. *Tectonophysics* 228, 471–463. https://doi.org/10.1016/0040-1951(93)90133-5

Roth Z. 1986: Kinematic model of tectonic development of the Carpathians and Alps in Cenozoic time. *Časopis pro mineralogii a geologii* 31, 1, 1–13.

Royden L.H., Horváth F. & Burchfield B.C. 1982: Transform faulting extension and subduction in the Pannonian region. *Geol. Soc. Amer. Bull.* 93, 717–725.

Simpson F. & Bahr K. 2005: Practical magnetotellurics. *Cambridge Univ Press*, 1–254. ISBN-0-521-817277

Sperner B., Ratschbacher L. & Nemčok M. 2002: Interplay between subduction retreat and lateral extrusion: Tectonics of the Western Carpathians. *Tectonics* 21, 6. 1051–1074. https://doi.org/10.1029/2001TC901028

Tomek Č. 1993: Deep crustal structure beneath the central and inner West Carpathians. *Tectonophysics* 226, 1–4, 417–431. https://doi.org/10.1016/0040-1951(93)90130-C

Tomek Č. & Hall J. 1993: Subducted continental margin imaged in the Carpathian of Czechoslovakia. *Geology* 21, 535–538. https://doi.org/10.1130/0091-7613(1993)021%3C0535:SCMIIN%3E2.3.CO;2

Tomek Č., Švancara J. & Budík L. 1979: The depth and the origin of the West Carpathian gravity low. *Earth Planet. Sci. Lett.* 44, 39–42.

Tomek Č., Ibrmajer J., Koráb T., Biely A., Dvořáková L., Lexa J. & Zbořil A. 1989: Crustal structures of the West Carpathian on deep reflection seismic line 2T. *Mineralia Slovaca* 21, 3–26 (in Slovak).

Varga G. & Lada F. 1988: Magnetotelluric measurement on the profile 2T. *Open file report*, *ELGI Budapest, Geofyzika Brno*, 1– 239.

Vozár J., Ebner F., Vozárová A., Haas J., Kovács S., Sudar M., Bielik M. & Pero C. 2010: Variscan and Alpine terranes of the Circum-Pannonian Region. *Geological Institute, SAS*, Bratislava, 1–233.

Supplement

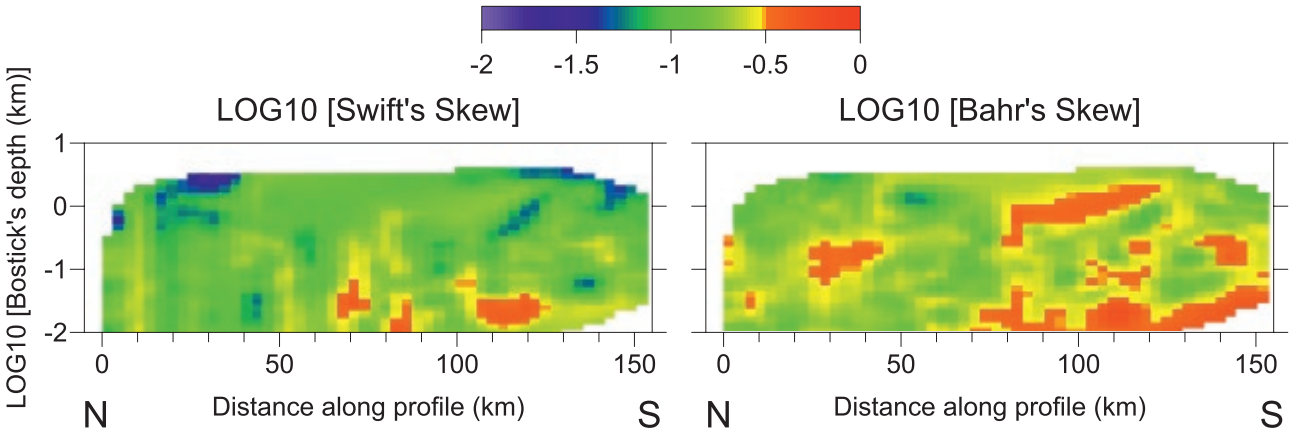

Fig. S1. Contour maps of the spatial distribution of the Swift's skew (left) and Bahr's phase sensitive skew (right) along the profile 2T and for various Bostick depths from the range of 0.1–100 km. Bostick depths are computed for Berdichevsky impedance invariants here, $Z_B=0.5(Z_{xy}-Z_{yx})$, and are mapping periods of the MT field, T in seconds, onto approximate penetration depths in the medium $Z_B=\{[\rho^a(T)T]/[2\pi\mu_0]\}^{0.5}$, in metres, where $\rho^a(T)$ is the apparent resistivity for the period of T (Bostick 1977).

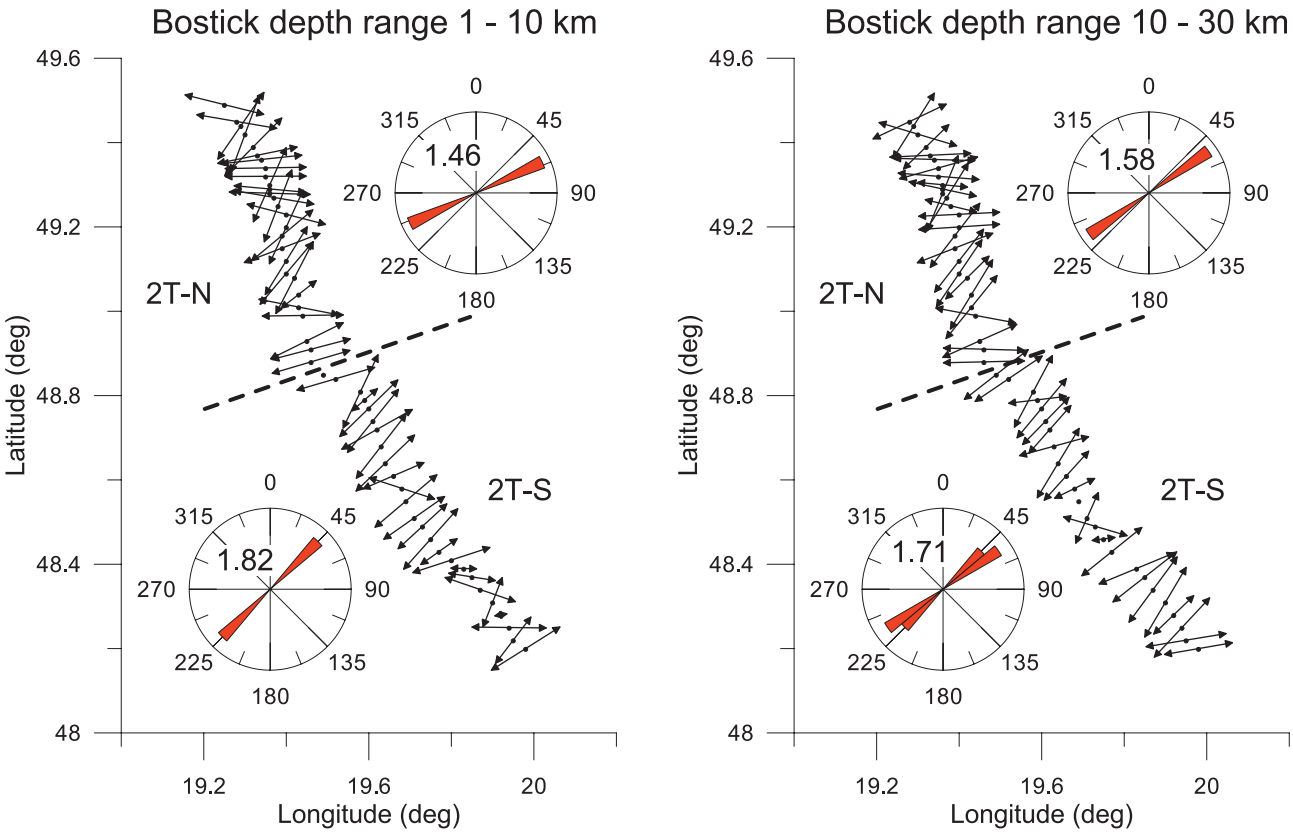

Fig. S2. Estimates of the regional strike from MT impedances based on Groom–Bailey decomposition within two Bostick depth ranges, 1–10 km (left) and 10–30 km (right). Arrows show regional strike estimates at individual sites on the 2T profile, the rose diagrams indicate a multisite strike estimates for the southern (2T-S) and northern (2T-N) sections of the profile. The labels in the rose diagrams show the RMS of the composite model fit to the observed impedances. The dashed line indicates a dividing line between the 2T-S and 2T-N profile sections.

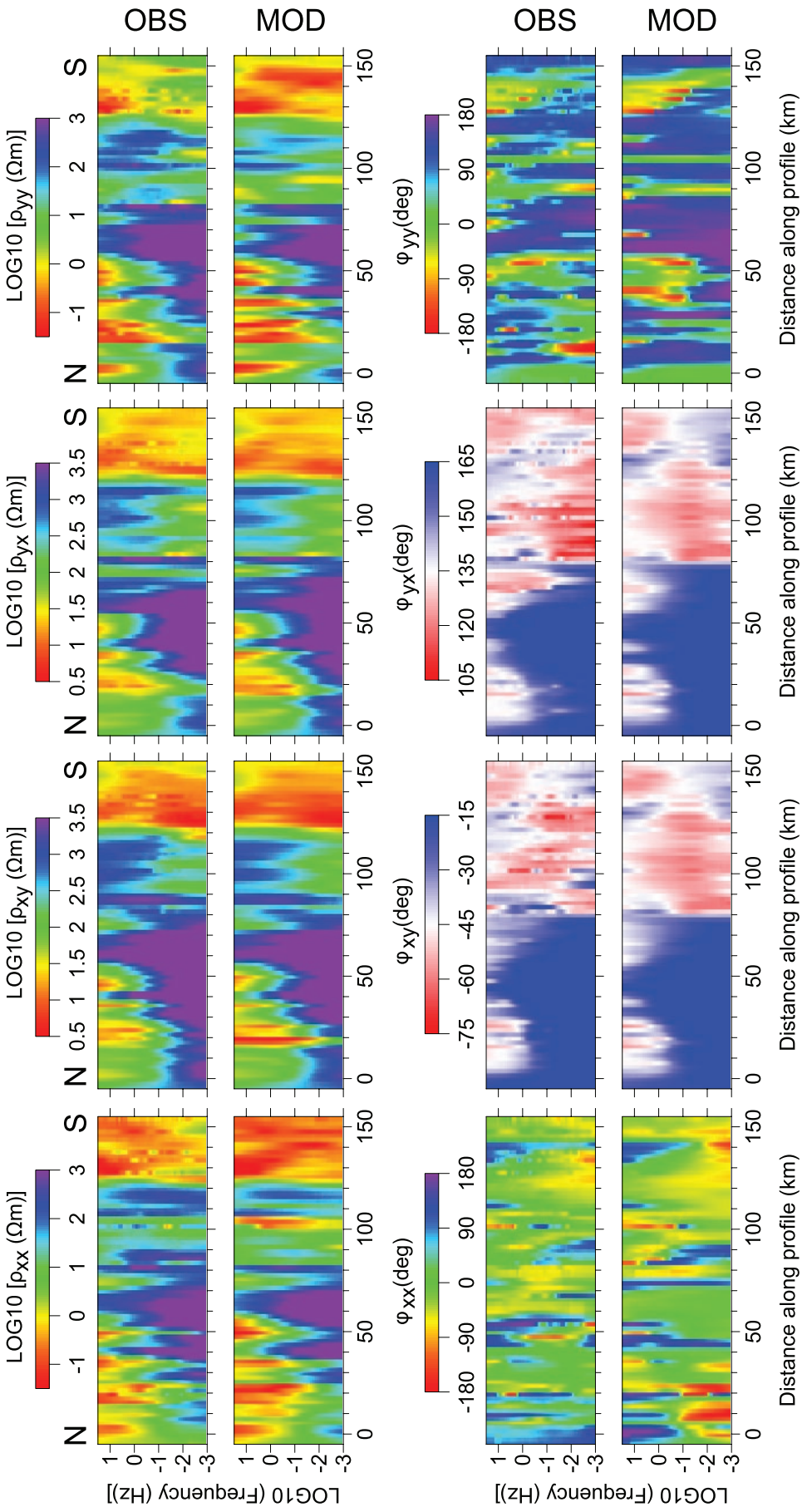

Fig. S3. Comparison of pseudosections of the apparent resistivities (top panels) and impedance phases (bottom panels) from the observed data (line OBS) and from model calculations (MOD). Resistivities and phases from all four impedance elements are shown, from left to right for *xx, xy, yx, yy*. The model data were rotated from their respective strikes in the N–E coordinate frame and then compared with the measured/processed parameters. Notice the changes in ranges for different parameters.